Attitude-Independent Magnetometer Calibration for Spin-Stabilized Spacecraft*

Gregory Natanson

a.i. solutions, Inc.
gregory.natanson@ai-solutions.com

ABSTRACT

The paper describes a three-step estimator to calibrate a Three-Axis Magnetometer (TAM) using TAM and slit Sun or star sensor measurements. In the first step, the Calibration Utility forms a loss function from the residuals of the magnitude of the geomagnetic field. This loss function is minimized with respect to biases, scale factors, and nonorthogonality corrections.

The second step minimizes residuals of the projection of the geomagnetic field onto the spin axis under the assumption that spacecraft nutation has been suppressed by a nutation damper. Minimization is done with respect to various directions of the body spin axis in the TAM frame. The direction of the spin axis in the inertial coordinate system required for the residual computation is assumed to be unchanged with time. It is either determined independently using other sensors or included in the estimation parameters. In both cases all estimation parameters can be found using simple analytical formulas derived in the paper.

The last step is to minimize a third loss function formed by residuals of the dot product between the geomagnetic field and Sun or star vector with respect to the misalignment angle about the body spin axis.

The method is illustrated by calibrating TAM for the Fast Auroral Snapshot Explorer (FAST) using in-flight TAM and Sun sensor data. The estimated parameters include magnetic biases, scale factors, and misalignment angles of the spin axis in the TAM frame. Estimation of the misalignment angle about the spin axis was inconclusive since (at least for the selected time interval) the Sun vector was about 15 degrees from the direction of the spin axis; as a result residuals of the dot product between the geomagnetic field and Sun vectors were to a large extent minimized as a by-product of the second step.

1. INTRODUCTION

The paper presents a new technique for calibrating a Three-Axis Magnetometer (TAM) on a spin-stabilized spacecraft. Contrary to the standard attitude-independent method solving only for magnetic biases, the developed 3-Step algorithm also solves for scale factors and misalignments (both orthogonal and non-orthogonal).

Due to the low cost of TAMs there is an increasing interest in using them as attitude sensors for both three-axis stabilized and spinning spacecraft. As a rule, ground TAM calibration prior to launch is insufficient, and the TAM has to be re-calibrated, using in-flight data. TAM calibration is a well-described technique[1,2] if three-axis attitude estimates are sufficiently frequent and accurate. However, in the case of spin-stabilized spacecrafts these high-frequency attitude estimates are usually not available. As a result, attitude-dependent calibration algorithms[1,2] become inapplicable.

Another TAM calibration procedure conventionally used both for three-axis stabilized spacecraft at an early stage of the mission and for spinning spacecraft involves the minimization of magnetic field magnitude residuals with respect to magnetometer biases.[3-8] An extension to this approach allowing for scale factors and nonothogonality corrections to be solved for has been suggested[9] but orthogonal misalignments of the TAM still remained undetermined.

*This work was supported by the National Aeronautics and Space Administration (NASA) / Goddard Space Flight Center (GSFC), Greenbelt, MD, USA, Contract NNG04DA01C.
NASA/GSFC, Mission Engineering and Systems Analysis Division, Flight Mechanics Symposium, Greenbelt, MD, Oct. 2005.

Section 2 presents the mathematical details of the three-step calibration algorithm. In Section 3, the method is illustrated by using in-flight TAM and Sun sensor data from the Fast Auroral Snapshot Explorer (FAST) mission.

2. THREE-STEP ESTIMATION OF TAM CALIBRATION PARAMETERS

The three-step TAM calibration algorithm, which (contrary to the standard technique[1,2]) treats orthogonal misalignments separately from scale factors and nonorthogonality corrections, is described in this section. The main difference between the two sets of calibration parameters is that errors in the TAM orientation do not affect the magnitude of measured magnetic field. For this reason one first has to estimate the deviations of scale factors and (if necessary) nonorthogonality corrections from their nominal values and only then (after re-adjusting the TAM measurements for the estimated errors) one can calibrate the TAM for the orthogonal misalignments. This sequence of calibration steps assures that re-adjustment of TAM measurements for orthogonal misalignments does not change magnitude residuals (which have been already minimized at the previous step).

The total (generally nonorthogonal) alignment matrix $\mathbf{M}$ is separated into symmetric and orthogonal parts, $\mathbf{S}$ and $\mathbf{O}$, namely,

$$\mathbf{M} = \mathbf{O}\,\mathbf{S}. \tag{1}$$

Diagonal elements of the matrix $\mathbf{S}$ account for scale factors whereas off-diagonal elements describe nonorthogonality corrections. Note that an arbitrary matrix $\mathbf{M}$ can always be decomposed into a product $\mathbf{O}\,\mathbf{S}$ of symmetric and orthogonal matrices:

$$\mathbf{S} = \sqrt{\mathbf{M}^T\mathbf{M}} \tag{2}$$

and

$$\mathbf{O} = \mathbf{M}\mathbf{S}^{-1}. \tag{3}$$

The three steps of the suggested calibration scheme can be summarized as follows. In Step 1 we estimate the symmetric matrix $\mathbf{S}$, together with TAM biases, by minimizing magnitude residuals. Steps 2 and 3 deal with estimation of the orthogonal alignment matrix $\mathbf{O}$. Step 2 is used to estimate the direction of the body spin axis in the TAM frame by minimizing residuals of the projection of the geomagnetic field onto the spin axis, under the assumption that spacecraft nutation has been already suppressed by a nutation damper. Finally, Step 3 deals with the misalignment of the TAM frame about the spin axis, which is estimated by minimizing residuals of the dot product between the Sun and geomagnetic field vectors. Alternatively one could minimize residuals of the angle between the Sun and magnetic field vectors. However, such a choice of the loss function has a certain deficiency for orbits with large eccentricity. In fact, to compute the angle, one first has to divide the dot product by the magnitude of the geomagnetic field. As a result, errors in the computed angle rapidly grow as the spacecraft approaches the orbit apogee.

The order of Steps 2 and 3 is essential. Since rotations around the spin axis do not affect the projection of the geomagnetic field on this axis, re-adjustment of TAM measurements at the last step does not change residuals minimized at Step 2.

The following subsections present the details of each of the three steps.

Step 1: Minimization of Magnitude Residuals (MMR)

The raw TAM measurements $\vec{B}^{\text{raw}}(t_k)$ with time tags t_k are adjusted via the relation:

$$\vec{B}^{\mathrm{TAM}}(t_k) = \mathbf{S}\left[\vec{B}^{\mathrm{raw}}(t_k) - \vec{b}\right], \tag{4}$$

where $\vec{b}$ is a vector composed of biases for each of the TAM axes and $\mathbf{S}$ is a 3x3 symmetric matrix. If the pre-launch calibration provides a nonorthogonal alignment matrix $\mathbf{M}_{\mathrm{nom}}$, then it can be also factored as $\mathbf{M}_{\mathrm{nom}} = \mathbf{O}_{\mathrm{nom}}\,\mathbf{S}_{\mathrm{nom}}$, where $\mathbf{O}_{\mathrm{nom}}$ is an orthogonal transformation from the nominal TAM frame to the body coordinate system (BCS). The symmetric matrix $\mathbf{S}_{\mathrm{nom}}$ and the pre-launch bias estimate $\vec{b}_{\mathrm{nom}}$ serve as a starting point for the matrix $\mathbf{S}$ and the vector $\vec{b}$. In the first-order approximation, the diagonal element S_{jj} of the symmetric matrix $\mathbf{S}$ describes a scale factor for the magnetometer axis j, whereas its off-diagonal elements $S_{jj'}$ (j>j'=1,2) are related to angles $\Phi_{jj'}$ between the axes j and j' via the relation: $\cos\Phi_{jj'} \approx 2\,S_{jj'}$.

Therefore $\vec{b}$ and $\mathbf{S}$ in Eq. (4) include pre-launch estimates $\vec{b}_{\mathrm{nom}}$ and $\mathbf{S}_{\mathrm{nom}}$ of biases, scale factors, and nonorthogonality corrections plus any post-launch adjustments to those nominal values. A general way of estimating these adjustments to $\vec{b}_{nom}$ and $\mathbf{S}_{\mathrm{nom}}$ is to minimize the loss function

$$L = \sum_k \left\{ \left| \mathbf{S}\left[\vec{B}^{\mathrm{raw}}(t_k) - \vec{b}\right] \right| - \left| \vec{B}^{\mathrm{I}}(t_k) \right| \right\}^2, \tag{5}$$

with respect to $\vec{b}$ and $\mathbf{S}$, using known reference vectors $\vec{B}^{\mathrm{I}}(t_k)$ in geocentric inertial coordinates (GCI).

To avoid calibration of magnetic torquer coupling coefficients, only time intervals without noticeable spikes in torquer magnetic moment are used. This allows contamination of magnetometer measurements due to torquer activity to be treated as noisy corrections to biases.

After the first step has been accomplished, the nominal (pre-launch) orthogonal alignment matrix $\mathbf{O}_{\mathrm{nom}}$ is used to rotate Eq. (3) into the BCS,

$$\vec{B}^{\mathrm{MMR}}(t_k) = \mathbf{O}_{\mathrm{nom}}\vec{B}^{\mathrm{TAM}}(t_k). \tag{6}$$

Note that the vectors $\vec{B}^{\mathrm{MMR}}$ are resolved in the BCS, and superscript 'MMR' simply indicates that TAM measurements $\vec{B}^{\mathrm{TAM}}$ in the TAM frame were obtained via Eq. (4) with the estimated values of $\vec{b}$ and $\mathbf{S}$ from the MMR. (Since calibration for misalignments of the TAM relative to the body axes has not been done yet, it is assumed that the TAM frame in question coincides with the nominal TAM frame defined by the alignment matrix $\mathbf{O}_{\mathrm{nom}}$.) TAM measurements adjusted in this way serve as the starting point for Steps 2 and 3 to determine the TAM orientation $\mathbf{O}_{\mathrm{mis}}$ relative to the nominal TAM frame.

Step 2: Estimation of Spin-Axis Misalignment in TAM Frame

The final adjustment of TAM observations relative to the BCS is done via the relation:

$$\vec{B}^{\mathrm{B}}(t_k) = \mathbf{O}\,\vec{B}^{\mathrm{TAM}}(t_k), \tag{7}$$

where $\mathbf{O} = \mathbf{O}_{nom}\mathbf{O}_{mis}$.
Let us represent the orthogonal matrix $\mathbf{O}$ as

$$\mathbf{O} = [\hat{P}_x^{TAM}, \hat{P}_y^{TAM}, \hat{P}_z^{TAM}]. \tag{8}$$

The purpose of Step 2 is to locate a misaligned direction of the body spin axis $\hat{P}_z^{TAM}$ in the TAM frame, while Step 3 estimates the misalignment component about this direction.

The second loss function is introduced as

$$L'(\Delta b, s_3, \hat{P}_z^{TAM}; \hat{n}_{spin}^{I}) = \sum_k \left[s_3 \vec{B}^{TAM}(t_k) \bullet \hat{P}_z^{TAM} - \Delta b - \vec{B}^{I}(t_k) \bullet \hat{n}_{spin}^{I} \right]^2 \tag{9}$$

which is minimized with respect to the scalar bias correction Δb, the scale factor s_3, and the direction $\hat{P}_z^{TAM}$ of the spin axis in the TAM frame, under the assumption that the direction of the spin axis in GCI, $\hat{n}_{spin}^{I}$, remains unchanged with time and has been independently estimated either using another pair of sensors or by combining partially calibrated TAM measurement vectors in Eq. (6) with Sun (or star) sensor measurements. Alternatively, one can treat the projections of the vector $\hat{n}_{spin}^{I}$ as additional estimation parameters and, in this case, Step 2 combines TAM-only single-axis attitude estimation with a partial TAM calibration.

Including the scale factor s_3 into the set of calibration parameters estimated in Step 2 makes it possible to solve the problem in an analytical form, whether $\hat{n}_{spin}^{I}$ is a known or solved-for vector. The appropriate analytical formulas are discussed in the Appendix. Assuming that Step 1 is sufficiently accurate, then both the scale factor correction $\Delta s_3 \equiv s_3 - 1$ and the bias correction Δb are expected to be negligibly small. If this is not the case, then one has to re-investigate the output from Step 1 and adjust the third diagonal element of the matrix $\mathbf{S}$ and the z-component of the vector $\mathbf{S}\vec{b}$ for the corrections Δs_3 and Δb from Step 2. One can then minimize the loss function in Eq. (5) only with respect to the two other scale factors and the x- and y-projections of the vector $\mathbf{S}\vec{b}$, and repeat Step 2. If necessary, additional iterations could be performed.

Note that the loss function in Eq. (9) explicitly assumes that the GCI direction of the body Z axis remains unchanged with time. This implies that the spacecraft is in the nominal mode and thus undergoes pure rotation. An extension of this algorithm to nonzero nutation angles is discussed in Ref. 10.
An intermediate set of partially adjusted vector measurements in the Spin Axis Frame (SAF)

$$\vec{B}^{SAF}(t_k) = \mathbf{A}_{123}(\phi, \theta, 0)\vec{B}^{TAM}(t_k) \tag{10}$$

is then introduced by defining the misalignment angles ϕ and θ via the relation:

$$\hat{P}_z^{TAM} = [\sin\theta, -\cos\theta\sin\phi, \cos\theta\cos\phi]^T. \tag{11}$$

The matrix $\mathbf{A}_{123}(\phi,\theta,0)$ in Eq. (10) is the 1-2-3 sequence of Euler rotations with angles ϕ, θ, and 0. The full transformation matrix $\mathbf{O}$ from the TAM frame to BCS can be written:

$$\mathbf{O} = \mathbf{A}_{123}(\phi,\theta,\psi) \equiv \mathbf{A}_3(\psi)\, \mathbf{A}_{123}(\phi,\theta,0)\,. \tag{12}$$

As the zeroth-order approximation to the third Euler angle ψ, one can use its nominal value ψ_{nom}, found from the 1-2-3 decomposition $\mathbf{A}_{123}(\phi_{nom}, \theta_{nom}, \psi_{nom})$ of the matrix $\mathbf{O}_{nom}$. The post-launch calibration of this misalignment component is discussed in Step 3.

Step 3: Estimation of Misalignment of TAM Frame About Spin Axis

The last step, which deals with residuals of the dot product between the Sun (or star) and magnetic field vectors, requires knowledge of accurate time-tags of the Sun (or star) slit sensor measurements. The pertinent loss function has the form:

$$L' = \sum_{\ell} \left[\hat{S}^{B}(t_\ell^*) \bullet \mathbf{A}_3(\psi) \vec{B}^{SAF}(t_\ell^*) - \hat{S}^{I}(t_\ell^*) \bullet \vec{B}^{I}(t_\ell^*)\right]^2 , \tag{13}$$

where $\hat{S}^{B}(t_\ell^*)$ is a Sun measurement vector in BCS, with time tags t_ℓ^*, $\hat{S}^{I}(t_\ell^*)$ is the reference Sun vector in GCI, $\vec{B}^{I}(t_\ell^*)$ and $\vec{B}^{SAF}(t_\ell^*)$ are magnetic field reference and partially adjusted (via Eqs. (4) and (10) above) TAM measurement vectors interpolated to the times of the Sun sensor measurements. Minimization of the loss function in Eq. (13) with respect to the Euler angle ψ is performed numerically.

Note that Step 3 fails when the Sun vector is either parallel or anti-parallel to the spin axis. One should thus expect large errors in estimated values of the Euler angle ψ when the Sun vector becomes perpendicular to the body XY-plane.

3. TAM CALIBRATION USING FAST IN-FLIGHT DATA

In this section we describe the results of applying the three-step calibration algorithm to actual in-flight data from the FAST spacecraft. The FAST is a spin-stabilized spacecraft with a spin rate of 12 revolutions per minute (RPM) about the Z-axis. It has an eccentric 350x4200 kilometers orbit around the Earth, with an 83-degrees (deg) inclination. The nominal direction of the spin axis is 3.5 deg south of the negative orbit normal. The onboard sensors include one Horizon Crossing Indicator (HCI), one Spinning Sun Sensor (SSS) of 0.5 deg resolution, one TAM of 1 milligauss (mG) resolution, and two electromagnetic torquers.

We used the 4-orbit time span of FAST data, described in more detail in a previous paper[11] on TAM-only attitude/rate determination for spin-stabilized spacecrafts. Since an analysis of torquer magnetic moments revealed no pronounced spikes, we disregarded any contamination of TAM measurements due to torquer activity.

The TAM calibration was done in the order specified in the previous section. First, the TAM was calibrated for biases and scale factors by minimizing the loss function in Eq. (5). (Pre-launch estimates are [0 0 0] for $\vec{b}_{nom}$ and the identity matrix for $\mathbf{M}_{nom}$.) As a necessary condition for this step to be successful, we required that the resultant magnitude residuals form a band with a nearly zero mean and a width of about 5 mG. The first step was also supposed to suppress pronounced orbit-dependent variations of magnitude residuals, which were observed for magnitude residuals of uncalibrated TAM measurements depicted in Fig. 1a. In addition, since the body Z-bias and the scale factor for the Z-component of TAM measurements were also estimated in Step 2, the calibration can be considered sufficiently accurate only if the corrections to the bias and the scale factor from Step 2 are small.

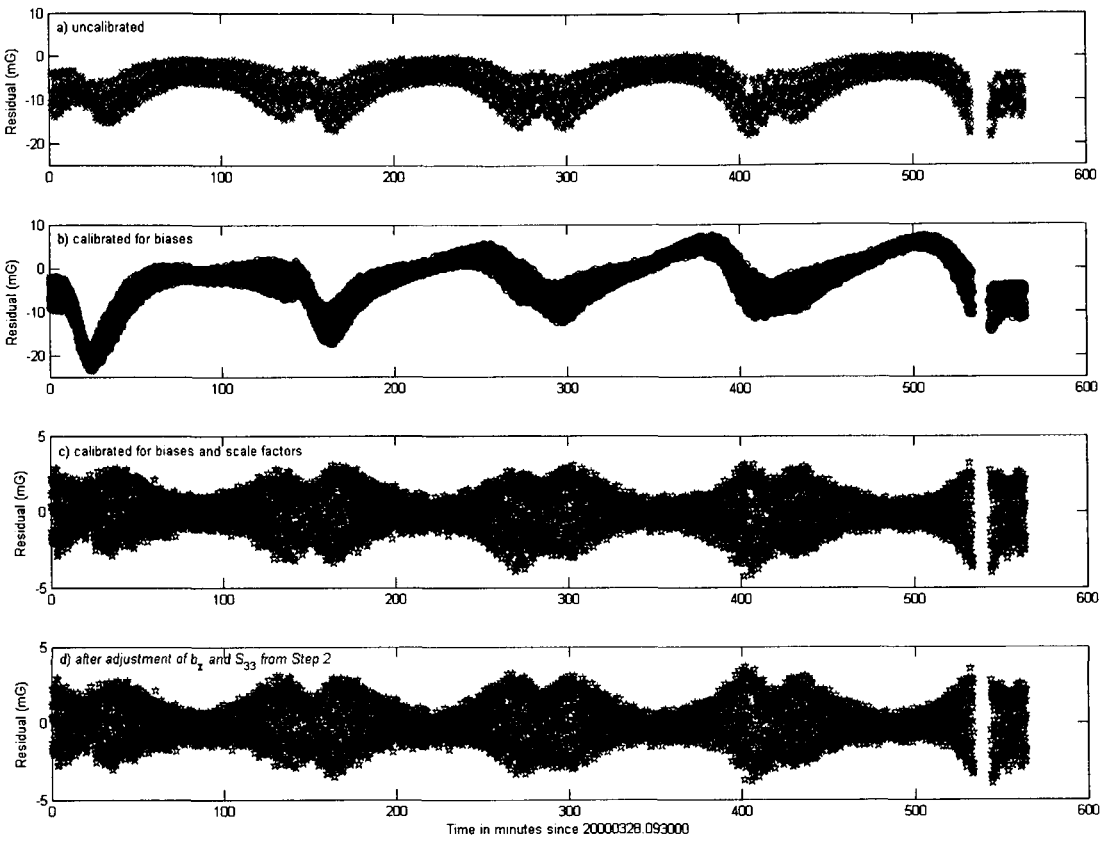

Figure 1. Magnitude Residuals of Measured Geomagnetic Field

One should also check the sensitivity of the Step 2 calibration parameters to the choice of the single-axis attitude solution for the direction of the spin axis in GCI , $\hat{n}^{I}_{spin}$. We used single-axis attitude solutions from the two conventional single-axis attitude estimation schemes: the SSS/HCI Earth-In Method[12] and the SSS/TAM Cone Method,[13] as well as instantaneous directions of the spin axis associated with three-axis attitude solutions from the SSS/TAM TRIAD.[14] Since both the SSS/TAM Cone Method and the SSS/TAM TRIAD initially use adjusted TAM measurements from Step 1, one has to assess how the Step 2 calibration affects the accuracy of these solutions.

Finally, one has to analyze residuals of the dot product between the Sun and geomagnetic field vectors. For this step it is essential that the SSS provides both the Sun angle (i.e., the angle between the Sun vector and the spacecraft Z-axis) and the time when the Sun entered the field of view (FOV) of the SSS. Using these observations, one can construct the necessary Sun vector measurements.

Evaluation of the three-step calibration algorithm was done for the TAM adjustment options listed in Table 1. First, we minimized the loss function in Eq. (5) with respect to only biases, since magnitude residuals are usually not sensitive to errors in scale factors and nonorthogonality corrections. However, as seen from Figures 1a and 1b, minimization of the Step 1 loss function only with respect to biases made errors in magnitude residuals near the orbit perigee even more pronounced, while giving an anomalously large value of -29.5 mG for b_z (Case b in Table 1). Magnitude residuals were uniformly reduced (see

Figure 1c) only after the loss function was minimized with respect to both biases and scale factors (Case c in Table 1) . An additional minimization of the Step 1 loss function with respect to off-diagonal elements of the matrix $\mathbf{S}$ did not produce reliable results and will be omitted from this discussion.

Table 1. TAM Adjustment Options

Description	Case	$[b_x, b_y, b_z]$ (mG)	$[S_{11}, S_{22}, S_{33}]$	ϕ, θ (deg)
no adjustment	a	[0, 0, 0]	[1, 1, 1]	0, 0
only for biases from Step 1	b	[-0.47, 1.62, -29.52]	[1, 1, 1]	0, 0
for biases and scale factors from Step 1	c	[-0.74, -2.01, 5.77]	[1.041, 1.022, 1.024]	0, 0
corrections to Case c from Step 2 (TRIAD)	d	[-0.74, -2.01, 4.27]	[1.041, 1.022, 1.039]	0, 0
TAM-only	e	[-0.74, -2.01, 4.34]	[1.041, 1.022, 1.032]	0.70, -0.46

Cases d and e reflect re-adjustments based on calibration results from Step 2, which are summarized in Table 2. Since the bias and scale factor corrections Δb and Δs_3 turned out to be relatively large, we adjusted both the bias b_z and the diagonal element S_{33} for these corrections, re-adjusted TAM measurements via Eqs. (4) and (6), repeated Step 2, and confirmed that this re-adjustment did not affect previously estimated values of misalignment angles ϕ and θ.

The algorithm was implemented for the following two approaches described in the Appendix:

i) the GCI direction of the spin axis, $\hat{n}^{\mathrm{I}}_{\mathrm{spin}}$, is independently estimated using other sensors;

ii) the GCI direction of the spin axis, $\hat{n}^{\mathrm{I}}_{\mathrm{spin}}$, is estimated together with ϕ and θ, by minimizing the loss function in Eq. (10).

Table 2. Step 2 Calibration Results Using Different Attitude Estimation Methods

TAM Adjustment Option	Source of Spin Axis	Δb (mG)	Δs_3	ϕ, θ (deg)
Case c	SSS/TAM (Cone Method)	-1.80	0.039	0.69, -0.46
Case c	SSS/TAM (TRIAD)	-1.56	0.014	0.69, -0.46
Case c	TAM-only	-1.48	0.013	0.67, -0.28
Case d	SSS/TAM (TRIAD)	0.00	0.000	0.70, -0.46
Case d	TAM-only	0.07	-0.007	0.70, -0.46
Case e	TAM-only	0.00	0.000	0.70, -0.46

Implementation of the first option was done using the three attitude estimation methods mentioned above: the SSS/HCI Earth-In Method,[12] the SSS/TAM Cone Method,[13] and the SSS/TAM TRIAD.[14] Case d in Table 1 describes the bias and scale factor re-adjustments based on the bias and scale factor corrections Δb and Δs_3 from Step 2, which was implemented using the TRIAD solution for $\hat{n}^{\mathrm{I}}_{\mathrm{spin}}$, with the Case c option for adjusted TAM measurements. Case e corresponds to the final output from the TAM-only version of the algorithm, which practically converged after the first iteration.

Note that both the TRIAD and the Step 3 calibration require interpolation of TAM measurement vectors to times of Sun sensor measurements. Since FAST is doing 12 revolutions per minute, X and Y components of the measured geomagnetic field rapidly oscillate, and the standard interpolation schemes do not work. For FAST we took advantage of the fact that the spacecraft rotates with a nearly constant rate, by interpolating projections of measured vectors onto the axes of the so-called 'despun' frame (which rotates

around the Z axis with the frequency of 12 Hertz) . The interpolated vectors were then rotated back to the BCS.

Table 3 compares mean GCI directions of the spin axis estimated using different attitude estimation methods. While predictions of the two single-axis attitude estimation methods for the GCI direction of the spin axis are relatively close, the TRIAD solution points about half a degree away. One might assume that discrepancies come from a TAM misalignment around the spin axis, which would result in large attitude errors re-distributed among all three axes. However, as discussed below, this is not the case, and TAM calibration has a very little effect on the estimated direction of the spin axis.

Table 3. Mean GCI Directions of Spin Axis From Different Attitude Estimation Methods

TAM Adjustment Option	Attitude Estimation Method	Right ascension (deg)	Declination (deg)
N/A	SSS/HCI	12.79	-11.34
Case c	SSS/TAM (Cone Method)	12.66	-11.24
Cases c and d	SSS/TAM (TRIAD)	13.03	-10.86
Case c	TAM-only	13.16	-10.71
Case d	TAM-only	13.12	-10.75
Case e	SSS/TAM (TRIAD)	13.05	-10.86
Case e	TAM-only	13.16	-10.75

Figure 2 depicts instantaneous GCI directions of the spin axis for each of the three methods, using adjusted TAM measurements from Case c. It is interesting that the line formed by solutions from the SSS/TAM Cone Model (despite a large spread of points along the line) goes directly through the spot formed by solutions from the SSS/HCI Earth-In Cone Method, whereas the spot formed by TRIAD solutions lies noticeably apart. As discussed below, calibration of TAM measurements for orthogonal misalignments reduced deviations of instantaneous directions of the spin axis from its mean position but had no significant effect on the estimated mean position.

The two attitude estimation schemes, the SSS/HCI Earth-In Method and the SSS/TAM TRIAD, also predict completely different patterns for deviations of the instantaneous direction of the spin axis from its mean position. As seen from Figure 3, the SSS/HCI Earth-In Method predicts a regular orbit-correlated motion of the spin axis around its mean position with relatively small nutation, whereas points associated with TRIAD solutions form a band. Step 2 calibration (using the Case e adjustment option) slightly reduces the band width, but does not change the pattern.

The simplest explanation for the discrepancy between the mean GCI directions of the spin axis predicted by the Single-Axis Attitude Estimation Methods and the TRIAD method is that a measured Sun angle has an undetected bias. This bias would have a much smaller effect on TRIAD solutions, because they are based on all three components of the measured Sun vector. Such an explanation is supported by the fact (see Table 3) that the TAM-only solution for the mean GCI direction of the spin axis is very close to that predicted by TRIAD. Bearing in mind that the SSS/HCI Earth-In Method[12] is an integral part of the application[15] used in Flight Dynamics operations for single-axis attitude validation, the discrepancy requires a more thorough investigation.

Since the calibration results given by Case e are based only on TAM measurements, this adjustment option was selected as a starting point for Step 3. Figure 4 illustrates the effect of calibration on residuals of the angle between geomagnetic field and the Sun vector. It is remarkable that these residuals became drastically smaller after Step 2, despite the fact that the loss function in Eq. (13) had not yet been minimized. Since Sun measurements have not been used for Case e, the small angle residuals serve as an additional argument in support of the calibration results.

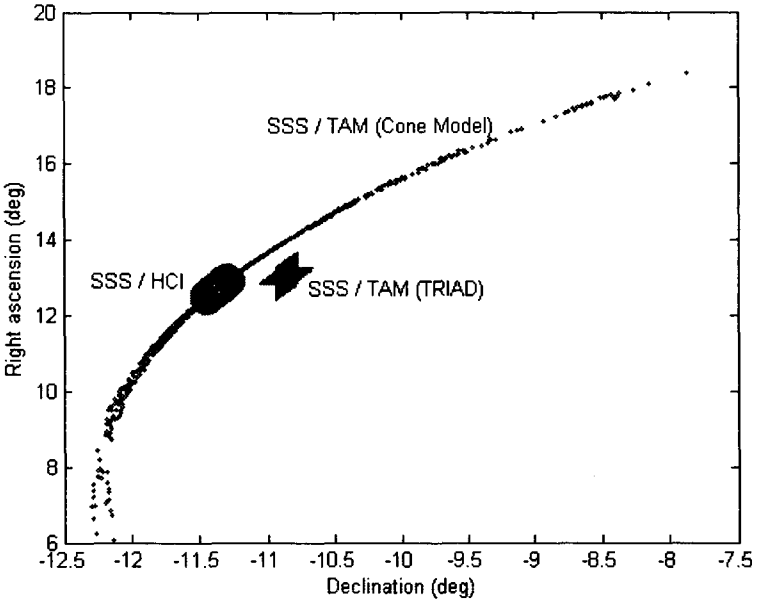

Figure 2. Estimated GCI directions of the spin axis using three different models: a) SSS/HCI Earth-In Method, b) SSS/TAM Cone Method, c) SSS/TAM TRIAD

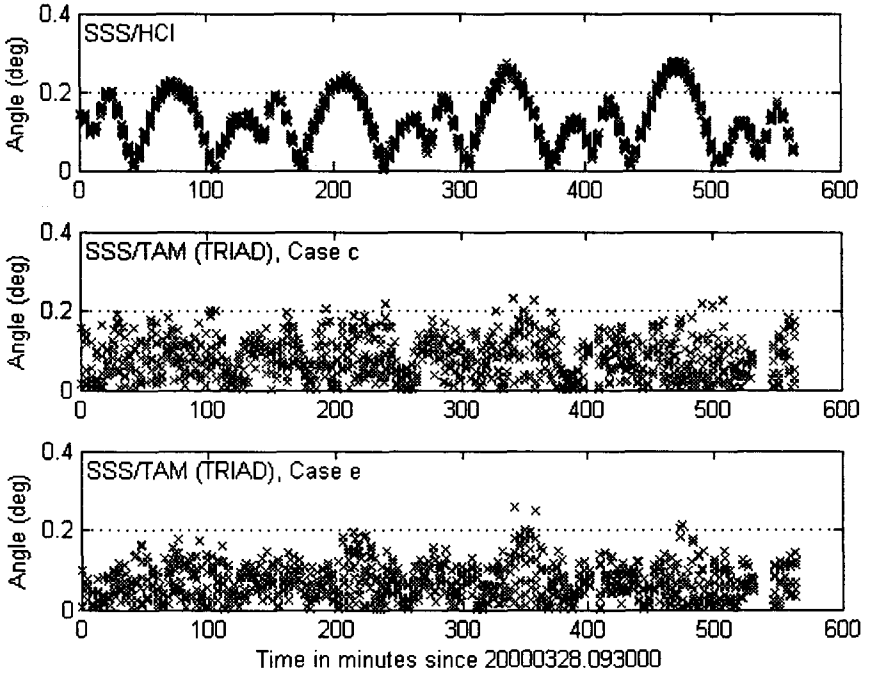

Figure 3. Angle between 'instantaneous' direction of the spin axis and its mean position

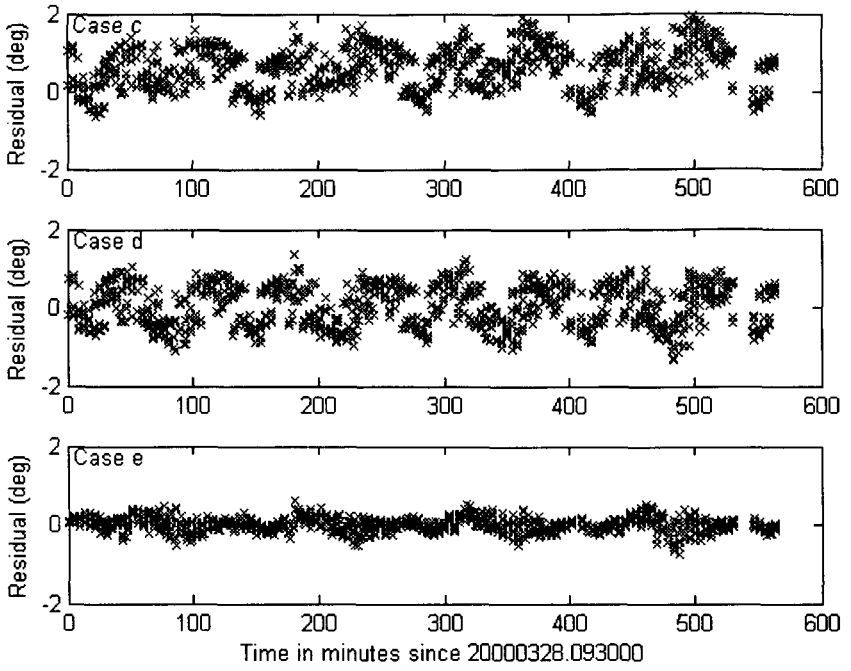

Figure 4. Residuals of the angle between the Sun vector and geomagnetic field

An attempt to further minimize these residuals using the Step 3 loss function did not produce any significant improvements in the resultant plot for the residuals. One should be careful, however, with final conclusions concerning the magnitude of the misalignment angle, taking into account that, during the selected time period, the Sun vector forms a relatively small angle (about 15 degrees) with the spin axis. As a result, the main contributions to the dot product between the geomagnetic field and the Sun vector come from the projection of the geomagnetic field on the spin axis, whose residuals were indeed minimized in Step 2. In other words, the relatively small angle between the Sun vector and the spin axis for this FAST data set negatively affects sensitivity of the Step 3 calibration. To clarify this point, Figure 5 depicts the RMS of the dot product between Sun and geomagnetic field vectors,

$$\text{RMS} = \sqrt{L'(\psi)/n} \tag{14}$$

as a function of all possible values of the misalignment angle ψ, where n is the number of good Sun measurements. As seen from the figure, there is a shallow minimum near $\psi \sim 0$, which is associated with uncertainties of a few tenths of degree in estimated angles of ψ. This implies that, for this FAST data set, Step 3 can estimate the TAM misalignment component about the spin axis only with the accuracy of about ± 0.5 degree. Case e can be thus considered as the final set of calibration parameters, which satisfies all of the specified validation criteria (except for the fact that TRIAD and TAM-only predictions for the mean GCI direction of the spin axis do not match those from Single-Axis Attitude Estimation Methods.)

4. CONCLUSIONS

The main purpose of the paper is to present a new attitude-independent TAM calibration algorithm for spin-stabilized spacecraft in the nominal mode and to evaluate its effectiveness, using spacecraft in-flight data. The most important result of the paper is a new tool for the attitude estimation of TAM orthogonal misalignments, which is achieved in Steps 2 and 3 of the developed 3-Step algorithm. Another important development is a Step 1 extension of the conventional scheme for attitude-independent estimation of

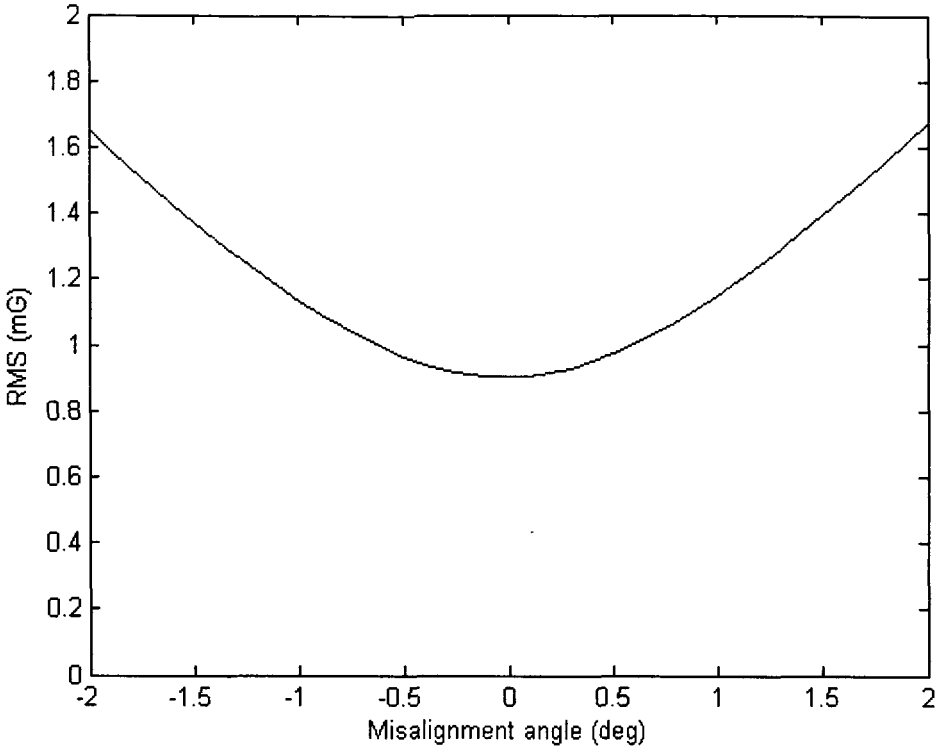

Figure 5. RMS of residuals of the dot-product between the Sun vector and geomagnetic field.

magnetic biases to include scale factors and nonorthogonality corrections into a set of estimated calibration parameters.

The algorithm was evaluated, using FAST in-flight data by comparing magnitudes of pre- and post-calibration TAM-only measurement residuals. Additional evaluation of the algorithm consisted of analyzing mutual consistency of the results from different calibration scenarios, as well as examining an effect of the TAM-only calibration on residuals of the angle between the measured Sun and geomagnetic field vectors .

Using these evaluation schemes, we concluded that the FAST TAM was successfully calibrated for three biases, three scale factor components, and two components of the orthogonal misalignment. It was demonstrated that the calibration only for biases exaggerated the relatively large errors in magnitude residuals near the orbit perigee and gave an anomalously large value for the Z-bias. This problem was eliminated after minimizing magnitude residuals with respect to both biases and scale factors. (Usually Step 1 allows one to estimate only biases. We found that the method was still not sensitive enough for reliable estimation of nonorthogonality corrections and the latter were simply neglected.) Based on results from Step 2, we also had to improve the body Z-bias and the scale factor for the third TAM axis. It was verified that these corrections did not have any noticeable effect on plotted magnitude residuals.

We found that the output from Step 2 (after the cited re-adjustment of the Z-component of TAM measurements) automatically took care of residuals of the angle between the Sun and magnetic field vectors. Solving for the misalignment about the spin axis in Step 3 thus turned out to be inconclusive (based on our evaluation data set). As explained in the paper, one of the reasons for such a relatively low

sensitivity of Step 3 is that the Sun vector is just 15 degrees from the spin axis during the selected time period.

We conclude that the new algorithm provides an effective tool for the in-flight calibration of TAMs on spin-stabilized spacecrafts in the nominal mode. It is recommended that the suggested three-step algorithm be used when TAM calibration is desired.

One remaining concern is the observed discrepancy between the mean GCI direction of the spin axis estimated via the Single Axis Attitude Estimation Methods and that estimated via TRIAD. This unresolved issue deserves more study.

Other suggestions for further study include:
(1) the extension[10] of the Step 2 algorithm making it possible to include nutation of an axially-symmetric spacecraft into the Step 2 loss function; (2) study of the sensitivity of Step 3 results at larger values of the angle between the Sun and magnetic field vectors.

ACKNOWLEDGEMENTS

The author is very grateful to J. Glickman and D. Weidow for numerous critical remarks and very productive suggestions, which significantly improved the quality of the paper.

APPENDIX

This appendix provides analytical formulas to minimize the loss function in Eq. (9) with respect to a bias correction Δb, the scale factor s_3, and the directions $\hat{P}_z^{TAM}$ of the body Z axis in the TAM frame for the known direction $\hat{n}_{spin}^{I}$ of the spin axis in the inertial coordinate system. If necessary, one can then substitute the derived explicit expressions of Δb, s_3, and $\hat{P}_z^{TAM}$ in terms of $\hat{n}_{spin}^{I}$ into the Step 2 loss function and find (also analytically) the absolute minimum of the latter function with respect to $\hat{n}_{spin}^{I}$.

Let us first exclude the bias correction Δb from Step 2 loss function, by nullifying the first derivative of L' with respect to Δb and then using the resultant relation to explicitly express Δb in terms of other estimation parameters:

$$\Delta b = \text{mean}\{\vec{B}^{TAM}(t_k)\} \bullet \vec{P}_z^{TAM} - \text{mean}\{\vec{B}^{I}(t_k)\} \bullet \hat{n}_{spin}^{I}. \qquad \text{(A1)}$$

The new loss function thus takes the form:

$$L'(s_3, \hat{P}_z^{TAM}; \hat{n}_{spin}^{I}) = \sum_k \left[s_3 \Delta\vec{B}^{TAM}(t_k) \bullet \hat{P}_z^{TAM} - \Delta\vec{B}^{I}(t_k) \bullet \hat{n}_{spin}^{I} \right]^2, \qquad \text{(A2)}$$

where we put

$$\Delta\vec{B}^{TAM}(t_k) \equiv \vec{B}^{TAM}(t_k) - \text{mean}\{\vec{B}^{TAM}(t_k)\} \qquad \text{(A3)}$$

and

$$\Delta\vec{B}^{I}(t_k) \equiv \vec{B}^{I}(t_k) - \text{mean}\{\vec{B}^{I}(t_k)\}. \qquad \text{(A4)}$$

Let us also introduce three auxiliary 3x3 submatrices:

$$\{\mathbf{f}_{TT}\}_{jj'} = \sum_k \Delta B_j^{TAM}(t_k)\,\Delta B_{j'}^{TAM}(t_k), \tag{A5}$$

$$\{\mathbf{f}_{TI}\}_{jj'} = \sum_k \Delta B_j^{TAM}(t_k)\,\Delta B_{j'}^{I}(t_k), \tag{A6}$$

and

$$\{\mathbf{f}_{II}\}_{jj'} = \sum_k \Delta B_j^{I}(t_k)\,\Delta B_{j'}^{I}(t_k), \tag{A7}$$

and represent the loss function given in Eq. (A4) in a simplified form:

$$L'(\vec{P}_z^{TAM}, \hat{n}_{spin}^{I}) = \vec{P}_z^{TAM} \bullet \mathbf{f}_{TT}\,\vec{P}_z^{TAM} + \hat{n}_{spin}^{I} \bullet \mathbf{f}_{II}\hat{n}_{spin}^{I} - 2\vec{P}_z^{TAM} \bullet \mathbf{f}_{TI}\hat{n}_{spin}^{I}. \tag{A8}$$

For each unit vector $\hat{n}_{spin}^{I}$, loss function (A8) has only one extremum with respect to $\vec{P}_z^{TAM}$ given by the linear equation:

$$\vec{P}_z^{TAM} = \mathbf{f}_{TT}^{-1}\,\mathbf{f}_{TI}\hat{n}_{spin}^{I}. \tag{A9}$$

If the direction $\hat{n}_{spin}^{I}$ is known, Eq. (A9) gives the estimation parameters in question: $s_3 = |\vec{P}_z^{TAM}|$ and $\hat{P}_z^{TAM} = \vec{P}_z^{TAM}/s_3$,

To minimize the loss function also with respect to $\hat{n}_{spin}^{I}$, one simply needs to substitute Eq. (A9) into loss function (A8), which gives

$$\tilde{L}'(\hat{P}_{z0}^{I}) = \hat{P}_{z0}^{I} \bullet \mathbf{F}\,\hat{P}_{z0}^{I}, \tag{A10}$$

where we put

$$\mathbf{F} \equiv \mathbf{f}_{II} - \mathbf{f}_{TI}\mathbf{f}_{TT}^{-1}\mathbf{f}_{TI}^{T}. \tag{A11}$$

The direction $\hat{n}_{spin}^{I}$ sought for must be either parallel or anti-parallel to the eigenvector $\vec{n}_{spin}^{I}$ of the matrix $\mathbf{F}$ associated with the lowest eigenvalue; that is,

$$\hat{n}_{spin}^{I} = \pm\,\vec{n}_{spin}^{I}/|\vec{n}_{spin}^{I}|. \tag{A12}$$

The sign in the latter expression should be chosen in such a way that the vector $\vec{P}_z^{TAM}$ found via Eq. (A12) forms an acute angle with the nominal direction of the body axis Z in the TAM frame (given by the third row of the nominal alignment matrix $\mathbf{O}_{nom}$). Finally the bias correction $\Delta\mathbf{b}$ is given by Eq. (A1).

REFERENCES

1. M. Challa and R. Harman, *A New Magnetometer Calibration Algorithm and Applications*, Proceedings of the AIAA Guidance, Navigation, and Control Conference, Boston, MA, August 10-12, 1998, pp. 697-707

2. M. Challa, *Algorithms for Attitude-Dependent Magnetometer Calibration in the Absence of Torquer Coupling*, CSC Technical Memorandum CSC-96-968-45, prepared for NASA-GSFC, October 2000

3. B. Gambhir, *Determination of Magnetometer Biases Using Module RESIDG,* CSC Report No. 3000-32700-01-TN, March 1975

4. R. H. Thomson, G.N. Neal, and M.D. Shuster, *Spin-Axis Attitude Estimation and Magnetometer Bias Determination for the AMPTE Mission*, Proceedings of the Flight Mechanics and Estimation Theory Symposium, NASA-GSFC, Greenbelt, MD, October 1981.

5. R. H. Thomson, G.N. Neal, and M.D. Shuster, *Magnetometer Bias Determination and Spin-Axis Attitude Estimation for the AMPTE Mission*, Journal of Guidance Control and Dynamics, Vol. 7, No. 4, 1984, pp. 505-507

6. P. B. Davenport, W.M.Rumpi, and G.L.Welter, *In-Flight Determination of Spacecraft Magnetic Bias Independent of Attitude*, Proceedings of the Flight Mechanics and Estimation Theory Symposium, NASA-GSFC, Greenbelt, MD, May 1988, pp. 326-343

7. R. Alonso and M.D. Shuster, *A New algorithm for Attitude-Independent Magnetometer Calibration*, Proceedings of the Flight Mechanics and Estimation Theory Symposium, NASA-GSFC, Greenbelt, MD, May 1994, pp. 513-527

8. J. Hashmall and J. Deutschmann, *An Evaluation of Attitude-Independent Magnetometer-Bias Determination Methods*, Proceedings of the Flight Mechanics and Estimation Theory Symposium, NASA-GSFC, Greenbelt, MD, May 1996, pp. 169-178

9. G. Natanson, *Attitude Independent Magnetometer Calibration Using Built-In MATLAB Functions,* CSC Technical Memorandum CSC-96-968-45, prepared for NASA-GSFC, October 2000

10. G. Natanson, *Early Mission Consistency Checks and Coarse Calibration of Three-Axis Magnetometers for Spin-Stabilized Spacecraft,* a.i. solutions Technical Memorandum FDF-88-010, prepared for NASA-GSFC, June 2005

11. M. Challa, G. Natanson, and N. Ottenstein, *Magnetometer-Only Attitude and Rate Estimates for Spinning Spacecraft,* AIAA/AAS Astrodynamics Specialist Conference, AIAA-2000-4241, Denver, Colorado, August 2000, pp. 311-317

12. J. R. Wertz (ed.), *Spacecraft Attitude Determination and Control*, D. Reidel Publishing Co., Dordrecht, Holland, 1985, pp. 355-359

13. Ibid., pp. 363–364

14. Ibid, pp. 424–426

15. N. Ottenstein et al., *Multi-Mission Spin Axis Stabilized Satellite (MSASS) Functional Specification*, Computer Sciences Corporation, CSC/TR-90/6051R1UD0, March 1993.